

Electronic Supplementary Information

Achieving Highly Stable Li-O₂ Battery Operations by Designing Carbon Nitride-Based Cathode towards Stable Reaction Interface

Peili Lou^{a,b}, Zhonghui Cui^{a,*} and Xiangxin Guo^{a,*}

^a State Key Laboratory of High Performance Ceramics and Superfine Microstructure, Shanghai

Institute of Ceramics, Chinese Academy of Sciences, Shanghai 200050, P. R. China

^b University of Chinese Academy of Sciences, Beijing, 100039, P. R. China

* Corresponding Author:

cuizhonghui@mail.sic.ac.cn (Z. H. Cui), xxguo@mail.sic.ac.cn (X. X. Guo)

Experimental Details

Synthesis of Mesoporous Boron-Doped C₃N₄ (m-BCN) The mesoporous boron-doped carbon nitride (m-BCN) was prepared by calcination the mixture of dicyandiamide and tetrafluoroborate-based ionic liquid (BmimBF₄) under air atmosphere [S1]. In a typical synthesis, 0.5 g of BmimBF₄ was dissolved in the distilled water (6 mL) and stirred for 5 min. Then 1 g of the dicyandiamide was added into the solution and the mixture was transferred to an oil bath and stirred under 100 °C until the water being completely evaporated. The resulted white solid was first calcined under 350 °C for 4 h and then under 550 °C for another 4 h, with a ramp rate of 2.3 °C/min in the whole process. After cooling down, the m-BCN sample was obtained. For comparison, the bulk C₃N₄ was synthesized *via* a well-established procedure by heating the dicyandiamide in a muffle furnace at 550 °C for 4 h with a ramp rate of 2.3 °C min⁻¹.

Preparation of the RuO₂@m-BCN The RuO₂@m-BCN composite was synthesized through a one-step solution method. In a typical synthesis, 0.5 g of the as-prepared m-BCN was dispersed in 100 mL of distilled water. After sonication for 1 h, 20 mL of RuCl₃ (0.025 M) solution was dropped into the m-BCN suspension and stirred for 2 h. Then 20 mL of NaBH₄ (0.2 M) solution was poured quickly into the suspension. After stirring at 25 °C for 1 h, the dark precipitates were collected, washed with distilled water thoroughly, and dried at 120 °C under vacuum for 24 h.

Material Characterization The microstructure was observed by using a transmission electron microscope (TEM, JEOL JEM-2100F TEM), where dark-field and bright-field scanning TEM (STEM) and energy-dispersive X-ray spectroscopy (EDS) elemental mappings were collected. The morphology was collected on a FEI Magellan 400 extreme high resolution scanning electron microscope (SEM). The X-ray diffraction (XRD) measurements were carried out on Bruker D2 X-ray diffraction. The surface and subsurface compositions of pristine samples were analyzed by

X-ray photoelectron spectroscopy (XPS, ESCALab-250) with an Al anode source. Nitrogen adsorption-desorption isotherms was measured on a Micrometitics Tristar 3000 system.

Electrochemical Characterization The cathodes were prepared by pressing the paste of RuO₂@m-BCN and PTFE binder with a weight ratio of 90:10 on a 10-mm-diameter stainless steel mesh (316L, 200 mesh, Alfa Aesar), and dried in vacuum at 100 °C for 12 h. The mass loading on each disk ranges from 3.8 to 5 mg cm⁻². The electrolytes used here were prepared by dissolving LiClO₄ (battery grade, Sigma-Aldrich) in DMSO (Sigma-Aldrich) with a concentration of 0.5 mol L⁻¹. To avoid the effects from trace water, the LiClO₄ was prebaked at 80 °C in vacuum for 48 h and the DMSO solvent was dried by freshly activated molecular sieves (4 Å type, Alfa Aesar) for more than one week. The final water content in DMSO was measured below 5 ppm by a Metrohm 831 KF Coulometer.

The Swagelok-type Li-O₂ cells were employed to study the electrochemical performance of the RuO₂@m-BCN composites. The cells were assembled in an argon-filled glove box (M-Braun, H₂O < 0.1 ppm, O₂ < 0.1 ppm), each of which includes a 0.5-mm-thick lithium anode, a glass-fiber (Φ12.5 mm, GF/B, Whatman) separator saturated with the 0.5 M LiClO₄-DMSO electrolytes (H₂O < 5 ppm), and a cathode. After assembly, the swagelok cell was sealed in a home-made airtight stainless-steel chamber with the inlet and outlet tubes for oxygen flowing. To eliminate the effect of trace water, the oxygen flowing was pre-purified by flowing through a tubular gas filter (40 mm in diameter and 350 mm in length) filled with freshly activated 4 Å molecular sieves. After 4 h rest, the cells were cycled on an Arbin BT2000 cycler.

The cyclic voltammetry (CV) was performed on a potentiostat/galvanostat instrument (Autolab, PGSTAT302N, Eco Chemie B.V.) utilizing a home-made three-electrode electrochemical cells, as previously reported [S2]. The working electrode was prepared by cast-coating a uniform

RuO₂@m-BCN ink onto the glass carbon electrode (Φ 3 mm). The mass loading of RuO₂@m-BCN was 100 $\mu\text{g cm}^{-2}$. All the CV tests were performed inside a Ar-O₂ (Ar : O₂ = 80: 20 vol %) filled glove box (Vigor Gas Purification Technologies Co. Ltd.), in which the water content is below 0.1 ppm.

Electrochemical Products Characterization The discharged and charged cathodes were taken out from the cells in a Ar-filled glove box, washed with CH₃CN (pre-purified with fresh activated molecular sieve, H₂O < 4 ppm) and dried under vacuum. The morphology variation upon cycling was visualized by scanning electron microscope (SEM, FEI Magellan 400). Products formed during cycling were analyzed by *ex situ* XRD, fourier transform infrared spectroscopy (FTIR, Tensor 27, Bruker), which was equipped inside an Ar prefilled glove-bag (Sigma-Aldrich), and XPS (ESCALab-250) with an Al anode source. The commercialized Li₂O₂ (Alfa Asear, 90%), LiOH (Alfa Asear, 99.995%) and Li₂CO₃ (Sigma, 99.999%) were used as reference. For XPS measurements, all the samples were pre-sputtered using 2 kV argon ions for 10 s. Note that for XPS, SEM and FTIR tests the samples were mounted quickly with less than 10 seconds exposing to the ambient air, but for XRD test, there was no exposing to the ambient air. For XRD tests, the cycled electrode was first saturated with paraffin oil to cut off the direct contact of product with atmosphere.[S3]

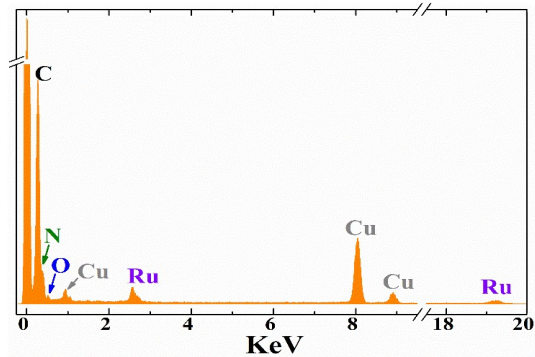


Figure S1. The EDX of the as-prepared RuO₂@m-BCN.

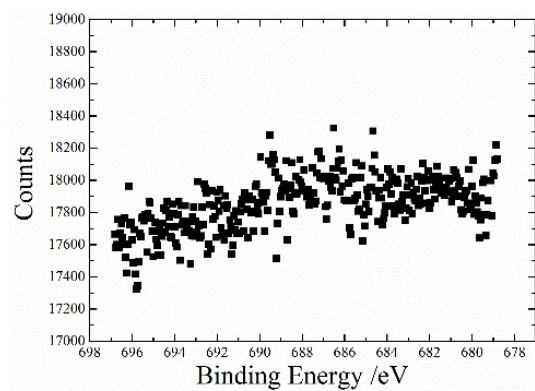


Figure S2. F 1s spectra of the RuO₂@m-BCN

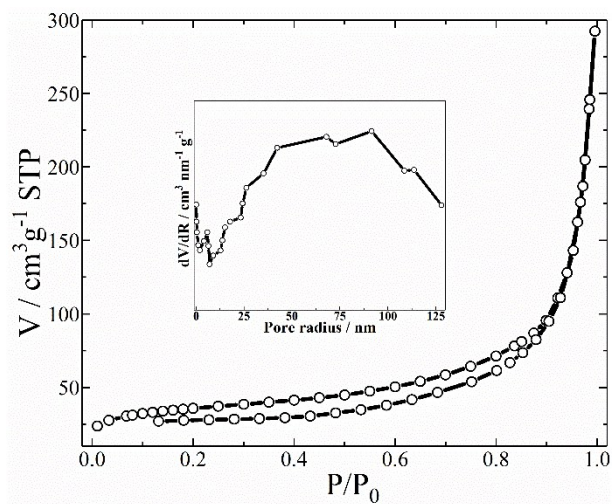


Figure S3. Nitrogen adsorption-desorption isotherms of the RuO₂@m-BCN. Inset shows the pore size distribution.

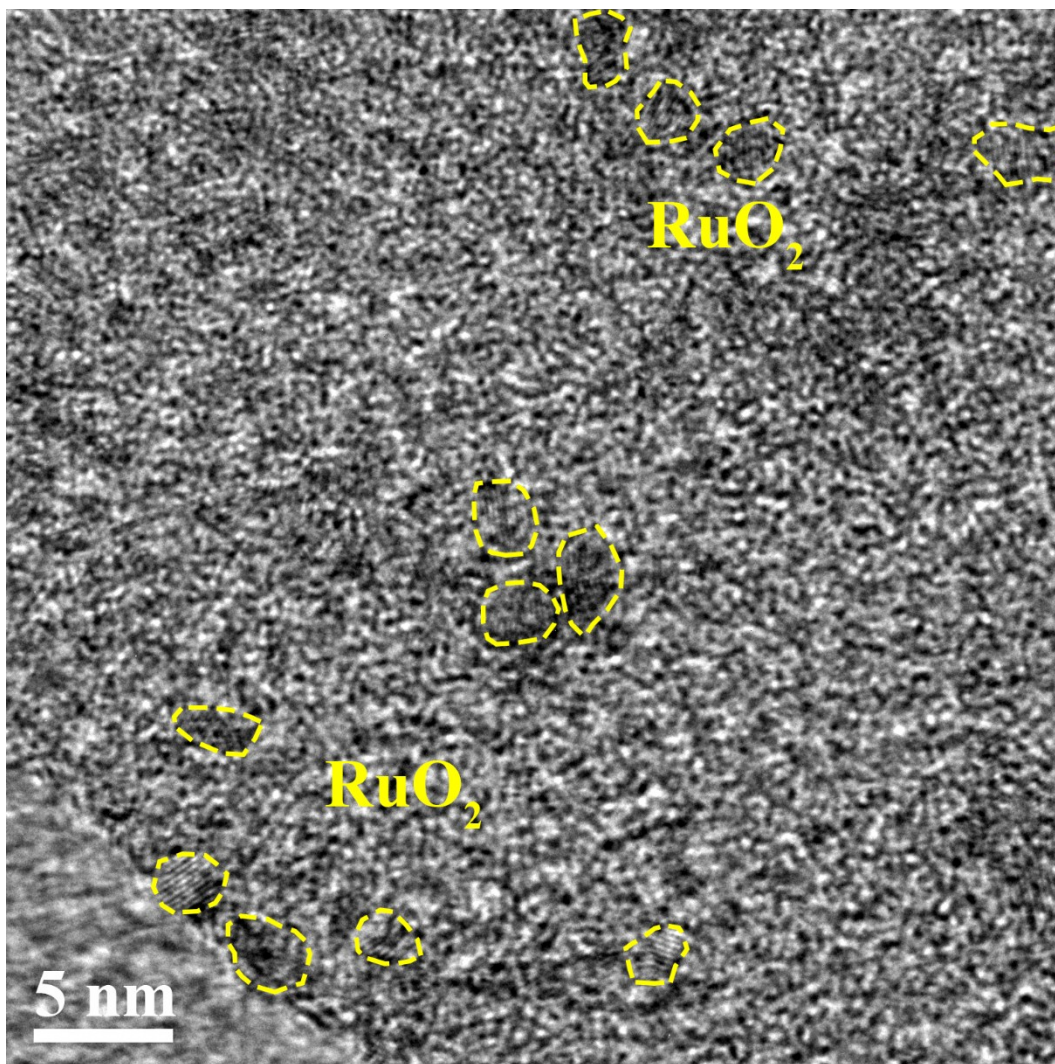


Figure S4. HRTEM of the RuO₂@m-BCN. Several typical RuO₂ nanocrystals (1-2 nm) are marked with yellow circles.

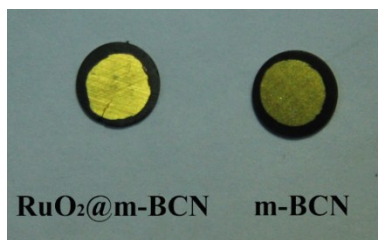


Figure S5. The photograph of the samples prepared for conductivity measurements. The diameter of Au electrode prepared by sputtering is 6 mm.

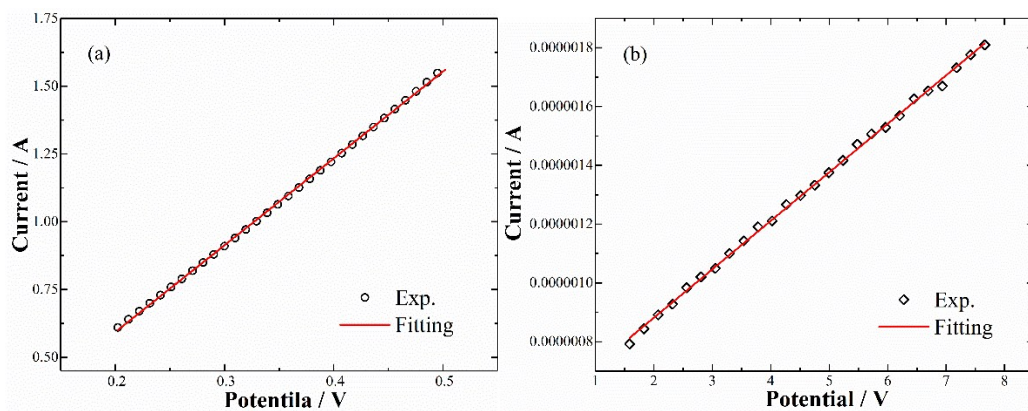


Figure S6. The I-V plots of the RuO₂@m-BCN (a) and m-BCN (b).

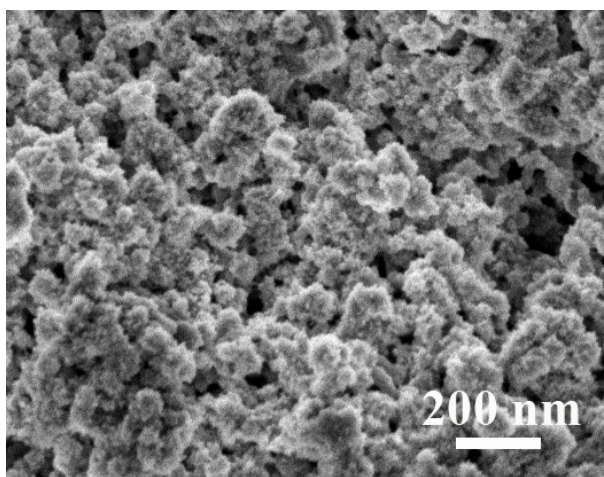


Figure S7. The morphology of the pristine RuO₂@m-BCN electrode.

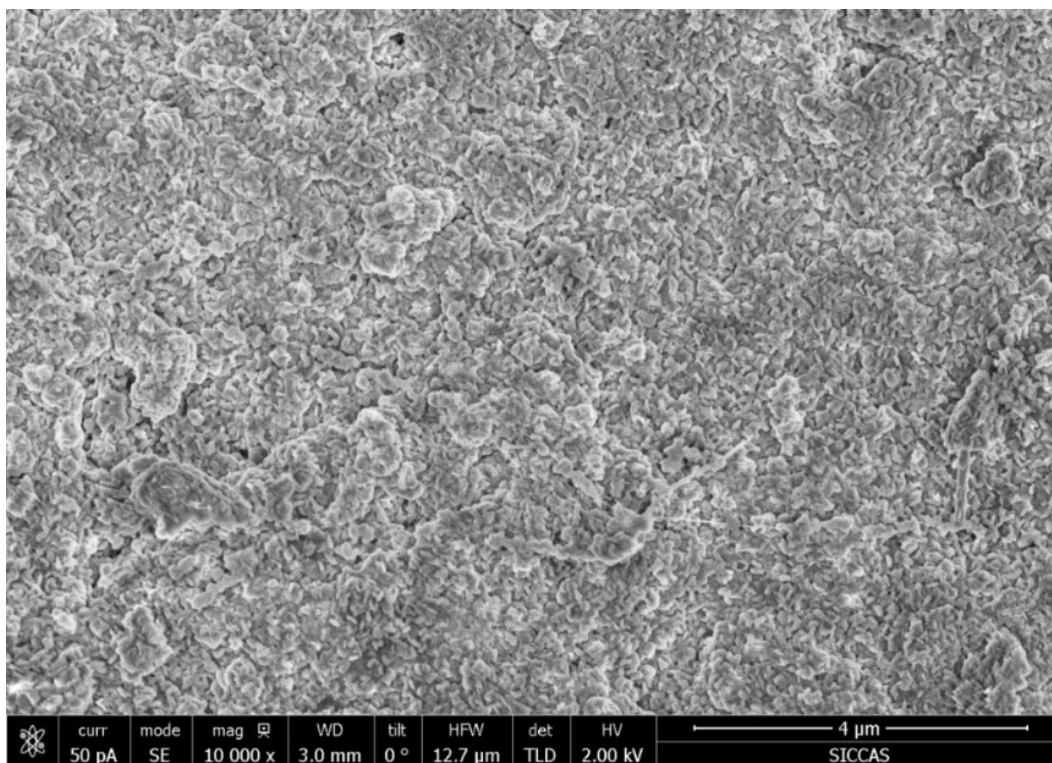


Figure S8. The morphology of the RuO₂@m-BCN electrode discharged at 0.2 mA cm⁻².

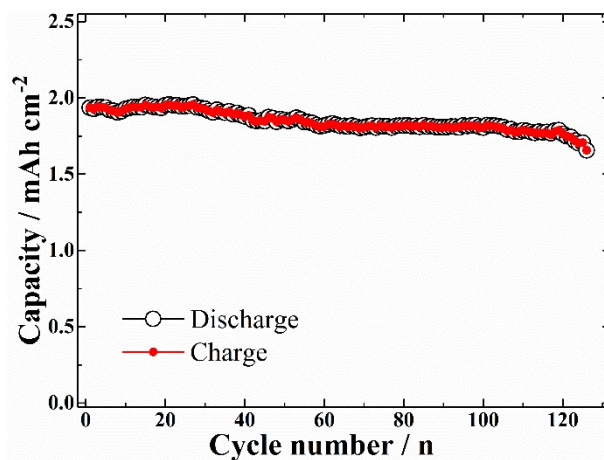


Figure S9. Cycle performance of the RuO₂@m-BCN at 0.3 mA cm⁻².

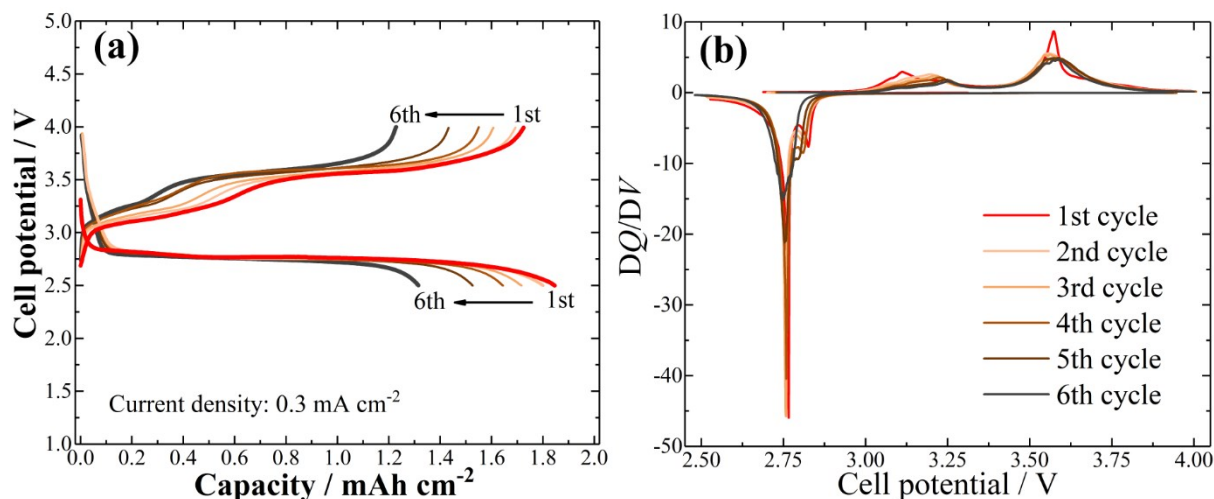


Figure S10. (a) Cycle performance of a RuO₂@m-BCN cathode operated between 2.5-4 V, (b) the corresponding dQ/dV curves.

Results and discussion: Figure S10 shows the cycle performance of a cell operated between 2.5 and 4 V. In the first two cycles, the cell behaves almost identical to that operated between 2.5 and 4.2 V. While from the third cycle, the discharge capacity decreases quickly from 1.808 to 1.31 mAh cm⁻² only after three cycles, indicating a poor cycle stability (Figure S10a). Meanwhile, the charging overpotential, especially for that of the slope region, increases accordingly from 0.165 to 0.3 V (Figure S10b). The main cause for this poor cycle performance may be the accumulation of by-products, which is supported by the absence of upward slope at around 4 V.

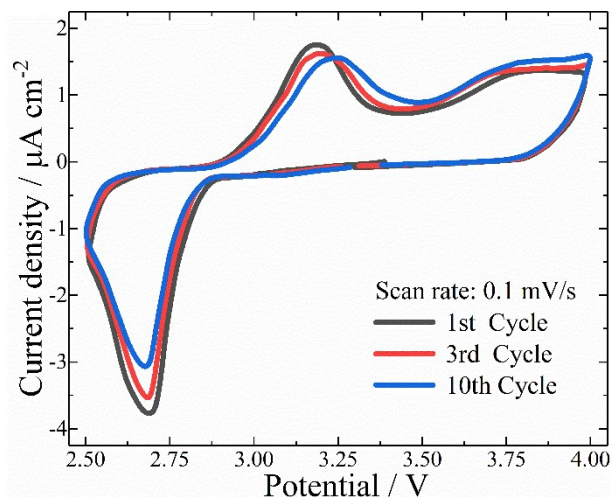


Figure S11. CV curves of the RuO₂@m-BCN collected in the voltage window of 2.5-4 V.

Results and discussion: Figure S11 shows the CV curves collected within the voltage range of 2.5-4.0 V. In the initial scan, the RuO₂@m-BCN shows almost same current response to that collected in a larger voltage window (Figure 3b). For example, an oxygen reduction peak corresponding to the formation of Li₂O₂ appears at 2.75 V during cathodic scan, and these discharge products are oxidized by a two-step OER process (*i.e.*, 3.125 and 3.75 V). Compared to the Figure 3b, there is no obvious oxidation peak occurred at the voltage cap (4 V), indicating the absence of high voltage induced electrolyte and/or by-product decomposition. However, the current responses corresponding to the Li₂O₂ formation (ORR) and decomposition (OER) show a gradual decrease as the increasing of cycle number, and the voltage gap between the ORR and OER peak increases accordingly. This clearly indicates the degradation of RuO₂@m-BCN during cycling, which is well consistent with the poor cycling performance observed in Figure S10. The main reason answering for this should be the passivation of RuO₂@m-BCN electrodes by the accumulated by-products during cycling.

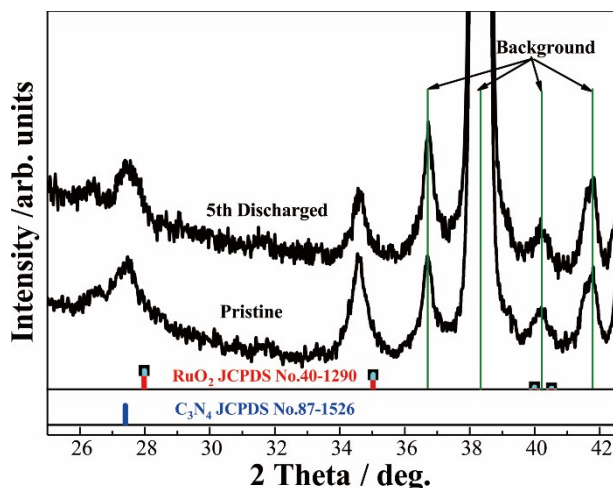


Figure S12. XRD patterns of the pristine and 5th discharged RuO₂@m-BCN electrode.

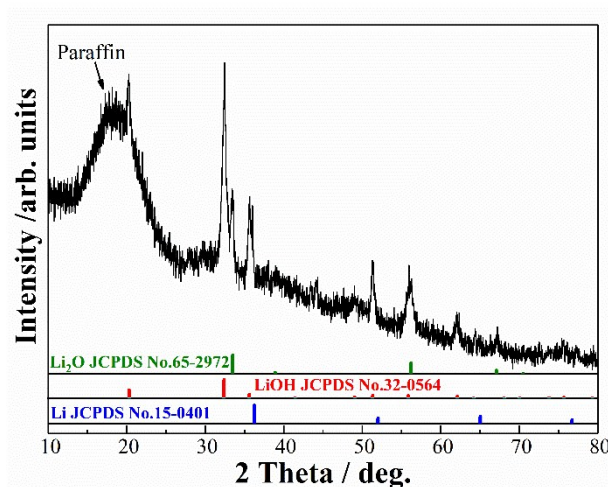


Figure S13. XRD pattern of a lithium anode collected from a failed Li-O₂ cell.

Results and discussion: Note that paraffin was employed as the protection layer to cut off further corrosion by ambient air, and the appearance of the lithium peaks in Figure S13 confirms that the cycled lithium anode is well-protected during XRD test. Figure S13 indicates that the lithium surface orienting to the electrolytes has changed into the mixture of LiOH and Li₂O. The Li₂O are formed from the oxidation of lithium by dissolved O₂. The formation of LiOH is related with the decomposition of DMSO. Among the commonly used electrolytes, the DMSO has a relatively

high donor number, meaning an enhanced stability upon oxygen radicals (*Science* 337, 2012, 563 and *ACS Appl. Mater. Interfaces* 2015, 7, 11402). However, it still suffers a time-dependent corrosion from super- or per-oxides, with LiOH as one kind of decomposition products (*J. Phys. Chem. Lett.* 2013, 4, 3115 and *J. Phys. Chem. Lett.* 2014, 5, 2850). The decomposition of such formed LiOH on recharge induces the formation of water (*Nat. Commun.* 2015, 6, 7843), which immediately dissolves in the DMSO and causes the lithium transformed into LiOH. In conclusion, the corrosion from dissolved oxygen and trace water derived from DMSO decomposition is the real reason for the lithium anode failure.

Table S1. The comparison of RuO₂@m-BCN with some previously reported carbon-free cathodes.

Cathode Materials	Discharge Capacity (mAh g⁻¹)	Cyclability	Rate capability	Ref.
Nanoporous Au	~ 320 @ 500 mA g ⁻¹	95% after 100 cycles	500 mA g ⁻¹	12
Ti₄O₇	~ 353 @ 200 μA cm ⁻²	With a capacity cutoff of 100 mAh g ⁻¹ , 95% remains after 40 cycles	200 μA cm ⁻²	19
TiC	~350 @ 1 mA cm ⁻²	98% after 100 cycles	1 mA cm ⁻²	20
Ru/ITO	1.81 mAh cm ⁻² @ 0.15 mA cm ⁻²	~93% after 50 cycles	0.15 mA cm ⁻²	23
B₄C	-	With a capacity cutoff of 100 mAh g ⁻¹ , 100% remains after 250 cycles	100 mA g ⁻¹	26
RuO₂@m-BCN	~ 512 @ 0.2 mA cm⁻²	Full discharge-charge, 91.5% after 120 cycles	~ 249 mAh g⁻¹ @ 1 mA cm⁻²	This work

References:

[S1] Y. Wang, J. Zhang, X. Wang, M. Antonietti and H. Li, *Angew. Chem. Int. Ed.* 49, (2010), 3356-3359

[S2] Z.H. Cui, X.X. Guo, *J. Power Sources*, 267, (2014), 20-25

[S3] B. D. Adams, C. Radtke, R. Black, M. L. Trudeau, K. Zaghbi and L. F. Nazar, *Energy Environ. Sci.*, 6, (2013), 1772-1778